Random walks in time-varying networks with memory

Bing Wang [1,*] Hongjuan Zeng,[1] and Yuexing Han [1,2,†]

[1]*School of Computer Engineering and Science, Shanghai University, Shanghai, P.R. China*

[2]*Shanghai Institute for Advanced Communication and Data Science, Shanghai University, Shanghai, P.R. China*

(Received 13 May 2020; accepted 1 December 2020; published 23 December 2020)

Random walks process on networks plays a fundamental role in understanding the importance of nodes and the similarity of them, which has been widely applied in PageRank, information retrieval, and community detection, etc. An individual's memory has been proved to be crucial to affect network evolution and dynamical processes unfolding on the network. In this work, we study the random-walk process on an extended activity-driven network model by taking account of an individual's memory. We analyze how an individual's memory affects random-walk process unfolding on the network when the timescales of the processes of the random walk and the network evolution are comparable. Under the constraints of long-time evolution, we derive analytical solutions for the distribution of walkers at the stationary state and the mean first-passage time of the random-walk process. We find that, compared with the memoryless activity-driven model, an individual's memory enhances the activity fluctuation and leads to the formation of small clusters of mutual contacts with high activity nodes, which reduces a node's capability of gathering walkers, especially for the nodes with large activity, and memory also delays the mean first-passage time. The results on real networks also support the theoretical analysis and numerical results with artificial networks.

DOI: 10.1103/PhysRevE.102.062309

I. INTRODUCTION

Random walks on networks describes a diffusion process, which has broadly been applied in ranking systems [1], community detection [2], and decision-making [3]. According to different rules, random walks in static networks can be divided into classical random walks [4], self-avoiding walks [5], biased random walks [6], and quantum walks [7]. Among them, the classical random walks, where walkers move to one of its neighboring nodes with equal probability has been widely studied.

In the early stage of network research, due to the limitations of data collection and storage equipment, a large amount of research work focused on static time-aggregated networks, in which edges between nodes do not change over time [8,9]. However, most complex systems in nature, society, and technology show temporal characteristics, where the pattern of connections between individuals evolves in time [10]. The increasingly accurate marking of temporal data facilitates the description of network structure [11,12].

Thus, more attention to random walks in time-varying networks has been paid with the help of the activity-driven network model [13]. In the activity-driven model, each node in the network is activated according to the preassigned activity which describes the propensity of the node to form connections. Although the model is simple, it describes the characteristics of temporality and degree distribution of real systems. Unlike annealed and quenched networks, random-walk diffusion process is affected by the temporal connectivity patterns between nodes [14–18], which means that walkers can get trapped at temporarily isolated nodes. It shows that nodes with large activity have strong ability to collect walkers and reduce the mean first-passage time (MFPT) [14]. By taking account of an individual's attractiveness, it shows that heterogenous attractiveness limits nodes' ability to collect walkers, especially when attraction and activity are positively correlated [16]. When links are established by the combination of node's fitness and activity, a nontrivial effect has been found on the properties of random-walk process [17]. The activity-driven model is further extended by considering burstiness [18–20], modularity [21], coupled structures [22], and multitype intetactions [23]. Interaction of nodes in groups of arbitrary numerosity is recently studied [24,25], which is modelled by simplex complexes [26,27] or hypergraphs [28].

In real networks, however, edges between nodes are not randomly connected as described in the activity-driven model but are affected by the non-Markovian effect due to an individual's memory [12,29,30]. Individuals tend to interact with people they already know, establishing strong or weak links with them, which can restrain rumor spreading [31]. A reinforcement process encoded with a measurable parameter of memory has been studied in recent work [32]. Limited by the long evolution of the network, memory reduces the threshold of the susceptible-infected-susceptible model and promotes epidemic spreading, which is same for susceptible-infected-recovered dynamics [33]. In addition, the model of second-order and even higher-order memory network is proposed by defining edge path, which may speed up or reduce the diffusion process and affect the community detection [34,35].

*bingbignwang@shu.edu.cn
†han_yx@i.shu.edu.cn

In this paper, we investigate the random-walk process on an extended temporal network based on the activity-driven model with an individual's memory [32]. This feature of memory accounts for the fact that social interactions are not randomly established but concentrated toward already contacted nodes. We study the random-walk process unfolding in activity-driven time-varying networks with a parameter β tuning the memory strength [33]. In the long-time limit, we find analytical solutions for W_a which describes the number of walkers in given node of activity a in the stationary state of random-walk process and the MFPT, respectively. When the random-walk process starts after a period of network evolution, the numerical simulation results agree well with theoretical analysis. Compared with the memoryless case, since an individual's memory enhances the activity fluctuation, making the average degree grow slower than the memoryless case, it reduces nodes' abilities of gathering walkers and delays the MFPT. We then study how memory affects the random-walk process in real systems. By comparing the random-walk process on the null model with real data set, we find that an individual's memory reduces a node's capability of gathering walkers, which is consistent with what is observed in synthetic networks.

The manuscript is organized as follows. In Sec. II, we introduce the time-varying network model with memory and describe the random-walk process. In Sec. III, we analytically derive the expressions for the distribution of walkers at the stationary state and the MFPT of the random-walk diffusing on the extended temporal network model with memory. In Secs. IV and V, we give simulation results on synthetic networks and real systems, respectively. Finally, in Sec. VI, we summarize our work.

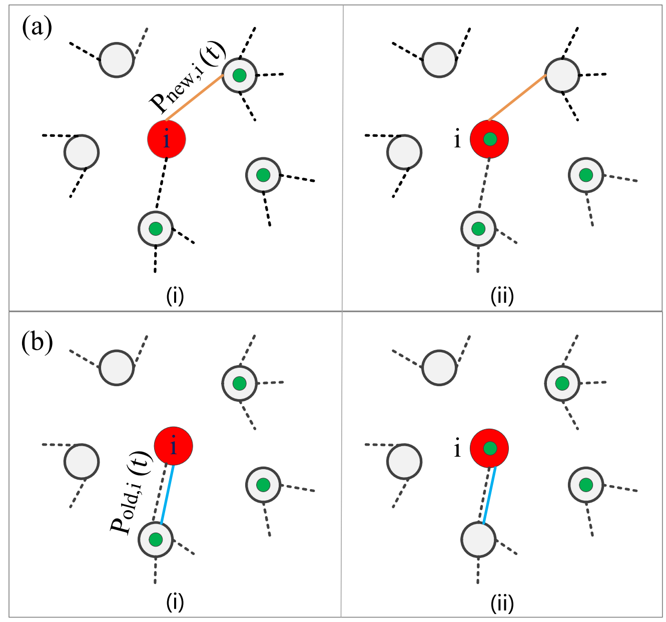

FIG. 1. Random walk in time-varying networks with memory. Panel (a) shows that with probability $P_{\text{new},i}(t)$, an active node i establishes a link with another node (at step 1) and walkers move along the link (at step 2). Panel (b) shows that with probability $P_{\text{old},i}(t)$, an active node i connects with an old neighbor (at step 1) and walkers move along the link (at step 2). Active and nonactive nodes are shown as red and gray nodes, respectively. Walkers are presented as fully green nodes. The edges between nodes already connected before are shown as gray dotted lines, and current contacts are shown as solid line. The green arcs with arrows represent the paths that walkers move.

II. MODEL

In the activity-driven framework, each node is characterized by a quenched, fixed activity a to establish contacts per unit time. To account for the observation that human behaviors are characterized by broad activity distributions, we consider a power-law distribution of activity $F(a) \propto a^{-\gamma}$ with $\varepsilon \leqslant a \leqslant 1$, where ε is a cutoff value that is chosen to avoid possible divergence of $F(a)$ close to the origin [13].

As shown in Fig. 1, at each time t, with probability $a_i \Delta t$, node i is activated. With probability $P_{\text{new},i}(t)$, it generates a new link to a new node that has never had a link to it, or with complementary probability $P_{\text{old},i}(t) = 1 - P_{\text{new},i}(t)$, it connects to an old one that has ever had a link to it until time t.

Empirical observations indicate that the probability for an individual that had interacted with $k_i(t)$ different individuals at time t to initiate a connection with a new individual is a function of $k_i(t)$. More precisely, the analysis of several data sets [32] has identified the relation

$$P_{\text{new},i}(t) = [1 + k_i(t)/c]^{-\beta}, \quad (1)$$

where $k_i(t)$ represents the number of distinct neighbors connected to node i until time t and the parameter $\beta > 0$ tunes the memory strength. The larger β is, the stronger the tie (the larger link-weight) between already-connected nodes will be. When $\beta \approx 0$, the probability $P_{\text{new},i}(t) \approx 1$ weakly depends on the growing degree $k_i(t)$. The constant c sets an intrinsic value for the number of connections that node i is able to engage in before memory effects become relevant [32]. The probability $P_{\text{new},i}(t)$ for node i to connect to a new node decreases as the degree $k_i(t)$ increases.

The generation process of the time-varying network with memory is demonstrated according to the following rules (see Fig. 1).

(i) At each discrete time step t, the network G_t starts with N disconnected nodes;

(ii) With probability $a_i \Delta t$, node i generates m links;

(iii) With probability $P_{\text{old},i}(t)$, nodes i connects with one of the $k_i(t)$ previously connected nodes, or with probability $P_{\text{new},i}(t)$, it connects to a new node j. Nonactive nodes can still receive connections from other active nodes.

(iv) At time $t + \Delta t$, the memory of each node is updated and the process starts over again to generate the network $G_{t+\Delta t}$.

Multiple edges and self-loops are not allowed. All the interactions have a constant duration Δt. Without loss of generality, in the following, we set $\Delta t = 1$.

The asymptotic form of the degree distribution in the time-varying network with memory can be derived analytically. In particular, in the regime $1 \ll k_i(t) \ll N$, the average degree $\bar{k}(a, t)$ of the nodes with activity a is narrowly distributed around the average value [32]

$$\bar{k}(a,t) = C(a)t^{1/(1+\beta)}. \quad (2)$$

The prefactor $C(a)$ is a function depending on the activity a and memory strength β that can be evaluated numerically by the condition

$$\frac{C(a)}{1+\beta} = \frac{a}{C^{\beta}(a)} + \int da \frac{F(a)a}{C^{\beta}(a)}. \quad (3)$$

Hereafter, we denote $g(a) = \frac{a}{C^{\beta}(a)}$, and $\langle g \rangle = \int daF(a)g(a)$ as the average of a function of $g(a)$ over the network. Hence, Eq. (3) can be written as:

$$\frac{C(a)}{1+\beta} = g(a) + \langle g \rangle. \quad (4)$$

Specifically, for $\beta = 0$, we have $C(a) = a + \langle a \rangle$ (the detailed derivation can be found in Ref. [32]).

III. ANALYTICAL RESULTS

We consider a Markovian and homogeneous random walk [14] unfolding on networks generated with the model as described above. We focus on the case where walkers move at the same time scale as the network evolution, i.e., at each time t, each walker moves from one node to another when a link presents beween them, as shown in Fig. 1. In the following, we derive the distribution of walkers W_a and the mean first-passage time MFPT at nodes with activity a, respectively.

A. The distribution of walkers W_a

The probability that the walker stays at node i at time t, $P_i(t)$, obeys the master equation, given by

$$P_i(t+\Delta t) = P_i(t)\left[1 - \sum_{j\neq i} \Pi_{i\to j}^{\Delta t}\right] + \sum_{j\neq i} P_j(t)\Pi_{j\to i}^{\Delta t}, \quad (5)$$

where $\Pi_{j\to i}^{\Delta t}$ is the probability that the walker moves from node j to node i during time interval Δt. The first term on the right-hand side represents the probability that the walker at node i at time t does not jump to other nodes at time $t + \Delta t$. The second term represents the probability that the walker at one of the node i's neighbors, j, at time t, moves to i at time $t + \Delta t$.

Let us define $\Omega_{i\to j}^{\Delta t}$ as the probability that node i becomes active and connects to node j, given as follows:

$$\Omega_{i\to j}^{\Delta t} = a_i m \Delta t \left\{ \frac{[1 - P_{\mathrm{new},i}(t)]A_{ij}(t)}{k_i(t)} + \frac{P_{\mathrm{new},i}(t)}{N - k_i(t) - 1} \right\}. \quad (6)$$

The first term represents that node i activates and selects acquaintance nodes to establish connections. The second term is due to that node i activates and creates a new connection. $A_{ij}(t)$ is the actual adjacency matrix of the network until time t, i.e., it is equal to 1 if node i and node j have been in contact at least once in the past and 0 otherwise. In this case, the instantaneous degree of node i is $k_i = m + \sum_j \Omega_{j\to i}^{\Delta t}$. Indeed, node i will generate m links and may potentially receive links from other active nodes.

Since both $A_{ij}(t)$ and $k_i(t)$ depend on the evolution time t, W_a, and MFPT will be affected by the starting time of the random-walk diffusion. The probability that node j is active and connects with node i is instead given by $\Omega_{j\to i}^{\Delta t} = a_j m \Delta t \{ \frac{[1-P_{\mathrm{new},j}(t)]A_{ij}(t)}{k_j(t)} + \frac{P_{\mathrm{new},j}(t)}{N-k_j(t)-1} \}$. In this case, the instantaneous degree of node i is $k_i = 1 + \sum_{l\neq j} \Omega_{l\to i}^{\Delta t}$. Here we assume that when node j is activated, a connection is established to node i. The former represents that node j becomes active and connects to node i, while the latter is that the activated nodes except node j establish links with node i.

Noting that the events described by $\Omega_{i\to j}^{\Delta t}$ and $\Omega_{j\to i}^{\Delta t}$ cannot happen at the same time. Moreover, according to the rules of random walk, a walker staying at node i randomly jumps to one of its k_i neighboring nodes. Putting them all together, in the limit $\Delta t \to 0$, the probability that a random walker moves from node i to one of its neighbors, j, $\Pi_{i\to j}^{\Delta t}$, can be written as

$$\begin{aligned}\Pi_{i\to j}^{\Delta t} &= \Omega_{i\to j}^{\Delta t} \frac{1}{m + \sum_j \Omega_{j\to i}^{\Delta t}} + \Omega_{j\to i}^{\Delta t} \frac{1}{1 + \sum_{l\neq j} \Omega_{l\to i}^{\Delta t}} \\ &\simeq a_i \Delta t \left\{ \frac{[1 - P_{\mathrm{new},i}(t)]A_{ij}(t)}{k_i(t)} + \frac{P_{\mathrm{new},i}(t)}{N - k_i(t) - 1} \right\} \\ &\quad + a_j m \Delta t \left\{ \frac{[1 - P_{\mathrm{new},j}(t)]A_{ij}(t)}{k_j(t)} + \frac{P_{\mathrm{new},j}(t)}{N - k_j(t) - 1} \right\},\end{aligned} \quad (7)$$

where we have neglected terms of order higher than Δt. The first (second) term in the first line (r-hand side) represents the probability that a walker moves from node i to j when the link is established by the active node $i(j)$.

Then, we can write the equation describing the evolution of $P_i(t)$ by substituting the expression $\Pi_{i\to j}^{\Delta t}$ and $\Pi_{j\to i}^{\Delta t}$ in Eq. (5):

$$\begin{aligned}\frac{\partial P_i(t)}{\partial t} =& -P_i(t) \sum_{j\neq i} \left(a_i \left\{ \frac{[1 - P_{\mathrm{new},i}(t)]A_{ij}(t)}{k_i(t)} + \frac{P_{\mathrm{new},i}(t)}{N - k_i(t) - 1} \right\} + a_j m \left\{ \frac{[1 - P_{\mathrm{new},j}(t)]A_{ij}(t)}{k_j(t)} + \frac{P_{new,j}(t)}{N - k_j(t) - 1} \right\} \right) \\ &+ \sum_{j\neq i} P_j(t) \left(a_j \left\{ \frac{[1 - P_{\mathrm{new},j}(t)]A_{ij}(t)}{k_j(t)} + \frac{P_{\mathrm{new},j}(t)}{N - k_j(t) - 1} \right\} + a_i m \left\{ \frac{[1 - P_{\mathrm{new},i}(t)]A_{ij}(t)}{k_i(t)} + \frac{P_{\mathrm{new},i}(t)}{N - k_i(t) - 1} \right\} \right).\end{aligned} \quad (8)$$

If the network evolves for a long time, the degree of node i follows $1 \ll k_i(t) \ll N$, i.e., each node has already had a large number of contacts, thus the probability that node i connects with new nodes can be ignored, while the network is still a sparse graph. In this limit case, we replace $N - k_i(t) - 1$ with N. By considering the leading terms, Eq. (8) can be rewritten as

$$\frac{\partial P_i(t)}{\partial t} = -P_i(t)\sum_{j\neq i}A_{ij}(t)\left[\frac{a_i}{k_i(t)}+\frac{ma_j}{k_j(t)}\right]+\sum_{j\neq i}P_j(t)A_{ij}(t)\left[\frac{a_j}{k_j(t)}+\frac{ma_i}{k_i(t)}\right]. \tag{9}$$

Furthermore, we perform equivalent analysis of the heterogeneous mean-field approximation for static networks, that is, we replace the time-integrated adjacency matrix $A_{ij}(t)$ with its annealed form, i.e., $Q_{ij}(t) = (1+\beta)t^{1/(1+\beta)}[g(a_i)+g(a_j)]/N$, which describes the probability that node i and node j have been in contact in the past [33]. We further replace $k_i(t)$ with $\bar{k}(a_i,t) = (1+\beta)(g(a_i)+\langle g\rangle)t^{1/(1+\beta)}$, and Eq. (9) can be written as

$$\frac{\partial P_i(t)}{\partial t} = -P_i(t)\sum_{j\neq i}\frac{1}{N}\left\{\frac{a_i[g(a_i)+g(a_j)]}{g(a_i)+\langle g\rangle}+\frac{ma_j[g(a_i)+g(a_j)]}{g(a_j)+\langle g\rangle}\right\}+\sum_{j\neq i}P_j(t)\frac{1}{N}\left\{\frac{a_j[g(a_i)+g(a_j)]}{g(a_j)+\langle g\rangle}+\frac{ma_i[g(a_i)+g(a_j)]}{g(a_i)+\langle g\rangle}\right\}. \tag{10}$$

We obtain a system-level description of the process by grouping nodes in the same activity a, assuming that they are statistically equivalent (mean-field assumption) [14]. Then, we define the number of walkers at a given node with activity a at time t as $W_a(t) = [NF(a)]^{-1}W\sum_{i\in a}P_i(t)$, where W is the total number of walkers in the system. By replacing the sums over nodes with integrals over the activities $1/N\sum_j U(a_j) \to \int U(a')da'F(a')$ and considering the continuous limit a, Eq. (10) can be rewritten as:

$$\begin{aligned}\frac{\partial W_a(t)}{\partial t} &= -W_a(t)\left[a+mg(a)\int\frac{a'F(a')}{g(a')+\langle g\rangle}da'+m\int\frac{a'g(a')F(a')}{g(a')+\langle g\rangle}da'\right]+g(a)\int\frac{a'F(a')W_{a'}(t)}{g(a')+\langle g\rangle}da'\\ &\quad+\int\frac{a'g(a')F(a')W_{a'}(t)}{g(a')+\langle g\rangle}da'+\frac{amg(a)}{g(a)+\langle g\rangle}\int F(a')W_{a'}(t)da'+\frac{am}{g(a)+\langle g\rangle}\int F(a')W_{a'}(t)g(a')da'\\ &= -W_a(t)\{a+[mg(a)\phi_1+m\phi_2]\}+g(a)\phi_3+\phi_4+\frac{amg(a)\omega}{g(a)+\langle g\rangle}+\frac{am}{g(a)+\langle g\rangle}\phi_5,\end{aligned} \tag{11}$$

where $\omega \equiv \frac{W}{N}$ is the average density of walkers per node, $\phi_1 = \int\frac{a'F(a')}{g(a')+\langle g\rangle}da'$ and $\phi_2 = \int\frac{a'g(a')F(a')}{g(a')+\langle g\rangle}da'$ are the coefficient of W_a, $\phi_3 = \int\frac{a'F(a')W_{a'}(t)}{g(a')+\langle g\rangle}da'$, $\phi_4 = \int\frac{a'g(a')F(a')W_{a'}(t)}{g(a')+\langle g\rangle}da'$ is the number of walkers that move to nodes with activity a due to the activation of other nodes, and $\phi_5 = \int F(a')W_{a'}(t)g(a')da'$ is the number of walkers that move to nodes with activity a as a consequence of the activation. The stationary state of the process is defined by the infinite time limit $\lim_{t\to\infty}\partial W_a(t)/\partial t = 0$. Using this condition in Eq. (11), we find the stationary solution

$$W_a = \frac{am\omega\frac{g(a)}{g(a)+\langle g\rangle}+g(a)\phi_3+\phi_4+\frac{am}{g(a)+\langle g\rangle}\phi_5}{a+mg(a)\phi_1+m\phi_2}. \tag{12}$$

Hence, we can see that the quantity W_a depends not only on the details of a node's activity but also on an individual's memory, controlled by $g(a)$. It is important to notice that at the stationary state ϕ_1, ϕ_2, ϕ_3, ϕ_4, and ϕ_5 are constants and they can be computed self-consistently by solving the following system of integral equations:

$$\begin{aligned}W &= N\int F(a)\frac{\frac{am\omega g(a)}{g(a)+\langle g\rangle}+g(a)\phi_3+\phi_4+\frac{am}{g(a)+\langle g\rangle}\phi_5}{a+mg(a)\phi_1+m\phi_2}da,\\ \phi_4 &= \int\frac{ag(a)F(a)}{g(a)+\langle g\rangle}\frac{\frac{am\omega g(a)}{g(a)+\langle g\rangle}+g(a)\phi_3+\phi_4+\frac{am}{g(a)+\langle g\rangle}\phi_5}{a+mg(a)\phi_1+m\phi_2}da,\\ \phi_5 &= \int g(a)F(a)\frac{\frac{am\omega g(a)}{g(a)+\langle g\rangle}+g(a)\phi_3+\phi_4+\frac{am}{g(a)+\langle g\rangle}\phi_5}{a+mg(a)\phi_1+m\phi_2}da.\end{aligned} \tag{13}$$

In the memoryless activity-driven (AD) networks, since edges between nodes are randomly selected, the W_a is given by [14]:

$$W_a = \frac{am\omega+\phi}{a+m\langle a\rangle}, \tag{14}$$

where $\phi = \int aF(a)W_a da$. We see that W_a only depends on the nodes' activity.

B. The MFPT

We now focus on another paramount property of random-walk process, i.e., the MFPT, defined as the average time steps needed for a walker to visit node i starting from an arbitrary node in the system [36].

Let us consider $p(i,n)$ as the probability that the walker reaches the target node i at time $t = n\Delta t$ for the first time. Then, $p(i,n)$ is simply given by

$$p(i,n) = \xi_i(1-\xi_i)^{n-1}, \tag{15}$$

where ξ_i is the probability that the walker jumps to node i during time interval Δt. The probability that a walker at node j jumps to node i during time Δt is given by $\Pi^{\Delta t}_{j\to i}$. Thus, we can write ξ_i as follows:

$$\xi_i = \sum_{j\neq i}\frac{W_j}{W}\Pi^{\Delta t}_{j\to i}, \tag{16}$$

where we replaced the probability that a single walker at node j at time t by its steady-state value with W_j/W.

The MFPT of node i can thus be estimated as follows:

$$\begin{aligned}\mathrm{MFPT}_i &= \sum_{n=0}^{\infty} \Delta t n p(i,n) = \frac{\Delta t}{\xi_i} = \frac{\Delta t}{\sum_{j\neq i} \frac{W_j}{W} \prod_{j\to i}^{\Delta t}} \\ &= \frac{W}{\frac{1}{N}\sum_j W_j \left\{ a_j \frac{g(a_i)+g(a_j)}{g(a_j)+\langle g\rangle} + a_i m \frac{[g(a_i)+g(a_j)]}{g(a_i)+\langle g\rangle} \right\}} \\ &= \frac{W}{g(a_i)\phi_3 + \phi_4 + \frac{a_i m g(a_i)}{g(a_i)+\langle g\rangle}\omega + \frac{m a_i}{g(a_i)+\langle g\rangle}\phi_5}, \end{aligned} \quad (17)$$

where ϕ_3, ϕ_4, and ϕ_5 are the three constants that can be calculated by Eq. (13). In numerical simulations, nodes are grouped in the same activity a, we have

$$\mathrm{MFPT}_a = \sum_{i\in a} \mathrm{MFPT}_i = \frac{W}{g(a)\phi_3 + \phi_4 + m\frac{ag(a)\omega + a\phi_5}{g(a)+\langle g\rangle}}. \quad (18)$$

The MFPT_a in the memoryless AD networks is given by [14]:

$$\mathrm{MFPT}_a = \frac{W}{ma\omega + \phi}, \quad (19)$$

where $\phi = \int aF(a)W_a da$. We see that the MFPT obtained in the AD network model is merely determined by node's activity.

It is worthing noting that, obviously, neither Eq. (14) nor Eq. (19) can be directly obtained from Eq. (12) or Eq. (17) by setting $\beta = 0$, since $P_{\mathrm{new},i}(t) = [1 + k_i(t)/c]^{\beta} = 1$, i.e., the activated node will definitely connect to a new node that has never had a link to, instead of randomly connecting to a node in the AD model.

IV. RESULTS ON SYNTHETIC NETWORKS

To support the results of the theoretical analysis, we have performed extensive Monte Carlo simulations of the random-walk process on the AD networks with memory. We consider a power-law distribution of activity, i.e., $F(a) \sim a^{-\gamma}$, with $a \in [10^{-3}, 1]$ and $\gamma = 2.1$. In each simulation, the temporal network evolves to time t_0 with the network average degree $\langle k\rangle_0$, which affects the time that the memory takes affects, then we start the random-walk process on it.

A. The distribution of walkers W_a

To verify the distribution of walkers W_a, networks are generated with size $N = 10^4$, $m = 6$, and the density of walkers is set as $\omega = 10^2$.

Since both the time of network evolution t_0, measured by $\langle k\rangle_0$, and the parameter β coaffect the memory strength, we first investigate how $\langle k\rangle_0$ affects W_a, as shown in Fig. 2. We also testify the effect of both weak memory [$\beta = 0.6$, Fig. 2(a)] and strong memory [$\beta = 3$, Fig. 2(b)] for different choices of $\langle k\rangle_0$, respectively. The results for the AD networks (red curve) are represented as the basin result. It shows that for all the cases with memory or without memory, the number

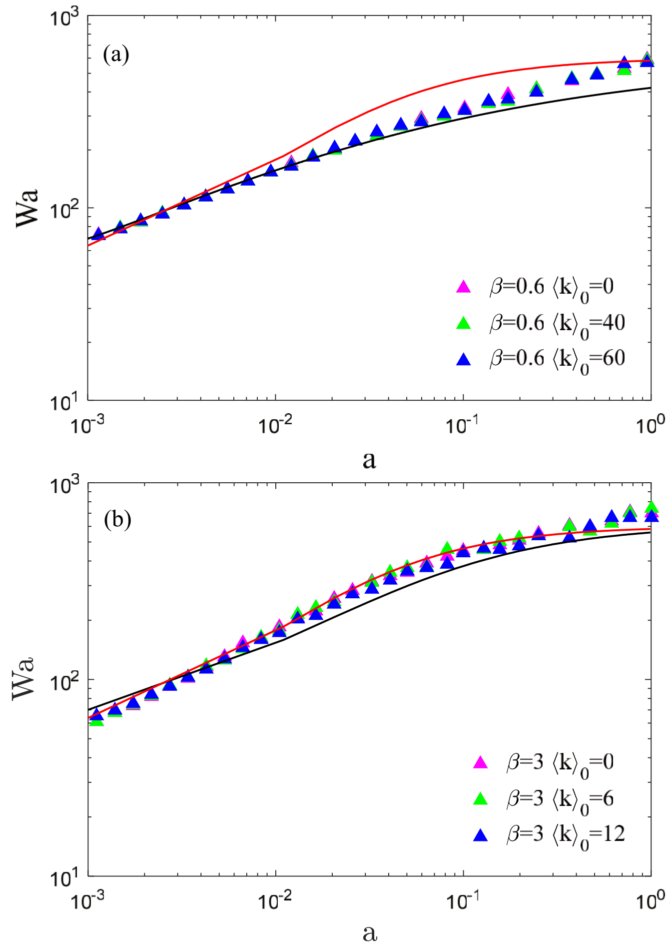

FIG. 2. The distribution of walkers W_a at nodes with activity a in networks with different memory strengths β and starting time t_0, measured by $\langle k\rangle_0$. The red curve and black curve represent theoretical predictions without [Eq. (14)] and with memory [Eq. (12)], respectively. Simulation results are shown as triangles. (a) Weak memory with $\beta = 0.6$; (b) strong memory with $\beta = 3$. Averages are performed over 500 independent simulations.

of walkers at nodes with activity a, W_a, increases with activity a monotonically. In other words, more walkers concentrate on highly active nodes. This result is expected, since more active nodes can build more links and receive more walkers from less active nodes, and vice versa. Therefore, the ability of a node to collect walkers strictly depends on its activity or its degree. As we know, due to the memory effect, nodes' degree grows slower than that without memory. As shown in Eq. (2), for the memory case, the average degree of the nodes with activity a grows as $\bar{k}(a,t) = C(a)t^{1/(1+\beta)}$, while it grows as $\bar{k}(a,t) \propto (a + \langle a\rangle)t$ for the memoryless case. Therefore, for $\beta > 0$, the number of walkers at nodes with activity a, W_a, is less than that with the memoryless case, especially for nodes with large activity, as shown in Figs. 2(a) and 2(b).

Next, we explore the impact of the average degree $\langle k\rangle_0$ on the distribution of walkers W_a. We find that the network evolution carried out in advance, determined by $\langle k\rangle_0$, has no obvious impact on W_a as shown in Figs. 2(a) and 2(b). In fact, for large $\langle k\rangle_0$, even if nodes obtained historical connections

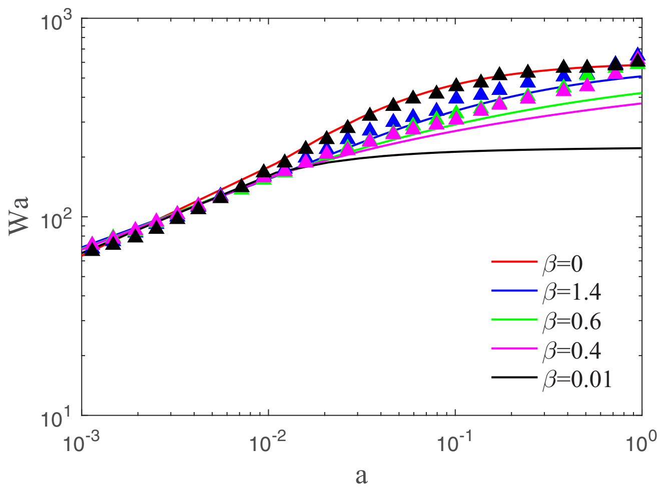

FIG. 3. The distribution of walkers W_a at nodes with activity a in networks for different choices of β with the same starting time t_0, measured by $\langle k\rangle_0 = 20$. The analytical results (continuous curves) and the numerical results (triangles) for the average number of walkers per node of class a are shown for $\beta = 0, 0.01, 0.4, 0.6, 1.4$. The red curve represents the theoretical prediction of W_a with Eq. (14), other curves are predicted with Eq. (12). All the results are the average over 500 independent simulations.

before the start of random-walk process, it takes long time for random-walk diffusion to reach a steady state, and the creation of new links takes effects on the random walks, thus eliminating the influence of $\langle k\rangle_0$ on W_a.

To further understand the memory effect in details, we explore the distribution of walkers W_a for diverse memory strength β as shown in Fig. 3. It shows that for an obvious memory strength (with $\beta > 0.4$), W_a increases with β for both simulation results (triangles) and theoretical results (solid curves). This phenomena demonstrates that with the strengthen of memory impact, i.e., with the increase of β, nodes with larger activity are more frequently connected with other nodes, and thus they can get more walkers from the process. In addition, we have to note that the gap between theoretical results and simulation results decreeases with β. The larger β is, the more consistent between theoretical and simulation results. This is due to the fact that when deriving W_a, we assume that $1 \ll k_i(t) \ll N$ for $i = 1, \dots, N$, where we ignored the creation of new links. However, for the special case of $\beta \to 0$ with $\beta = 0.01$, this assumption of ignoring new links connected by nodes is not true and it results in a great gap between analytical results (black solid curve in Fig. 3) and the simulation results (triangles).

B. The MFPT

We now turn our attention to the MFPT of random-walk process on the activity-driven networks with memory. We have performed Monte Carlo simulations to verify the theoretical results of the MFPT by setting the parameters as follows: $N = 3000$, $m = 6$, $W = 1$, $\gamma = 2.1$, where W is the number of walkers. Also in this case we start the random-walk process at t_0, where the average degree of the network is measured by $\langle k\rangle_0$.

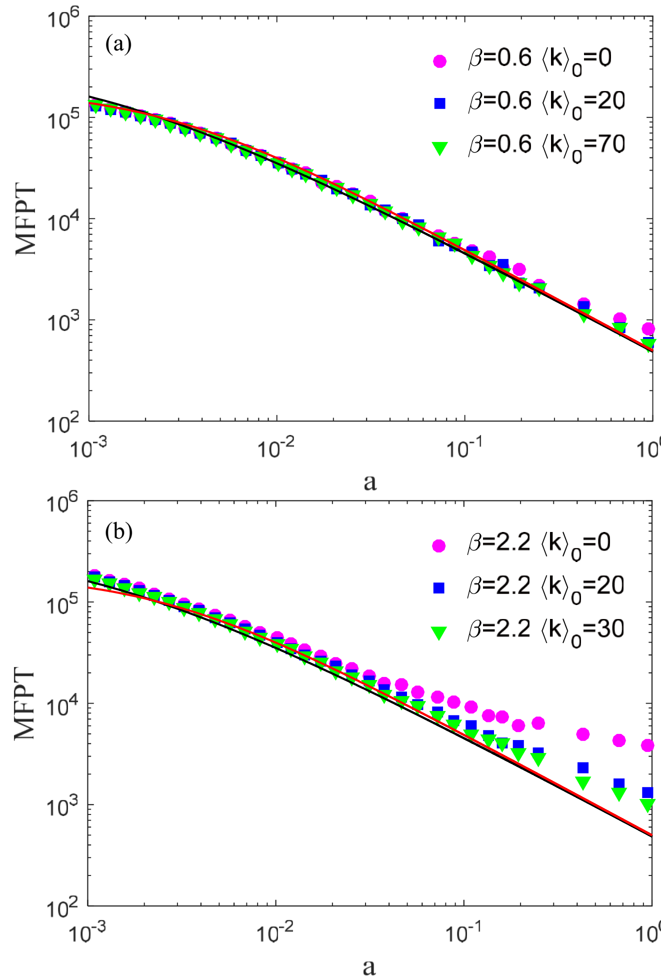

FIG. 4. The MFPT versus activity a for different $\langle k\rangle_0$. (a) $\langle k\rangle_0 = 0, 20, 70$; (b) $\langle k\rangle_0 = 0, 20, 30$. The red curve and black curve represent theoretical predictions without [Eq. (19)] and with memory [Eq. (17)], respectively. Simulation results are shown as symbols (dots, squares, and triangles). The network size is $N = 3000$ and $W = 1$. Each point is the average over 100 independent simulations.

First, we testify the coeffect of the memory strength β and $\langle k\rangle_0$ on the MFPT in Fig. 4. The memory strength is measured by weak memory [$\beta = 0.6$, Fig. 4(a)] and strong memory [$\beta = 3$, Fig. 4(b)] for different choices of $\langle k\rangle_0$, respectively. It shows that the MFPT decreases as activity a increases for all the memory strength we testified. Actually, nodes with large activity indeed have more connections, allowing walkers to reach them quickly.

Different from W_a, the MFPT depends on the average degree $\langle k\rangle_0$. As expected, the simulations of the MFPT approach toward to theoretical results as $\langle k\rangle_0$ increases, and this effect becomes more obvious with stronger memory strength with $\beta = 2.2$. In fact, compared to smaller $\langle k\rangle_0$, with larger $\langle k\rangle_0$, network evloves for longer time, where nodes got more historical links with the nodes that they have interacted, leading to the formation of large clusters. The larger clusters promote the reachability of walkers from one node to another, shortening the MFPT (Fig. 4, black curve).

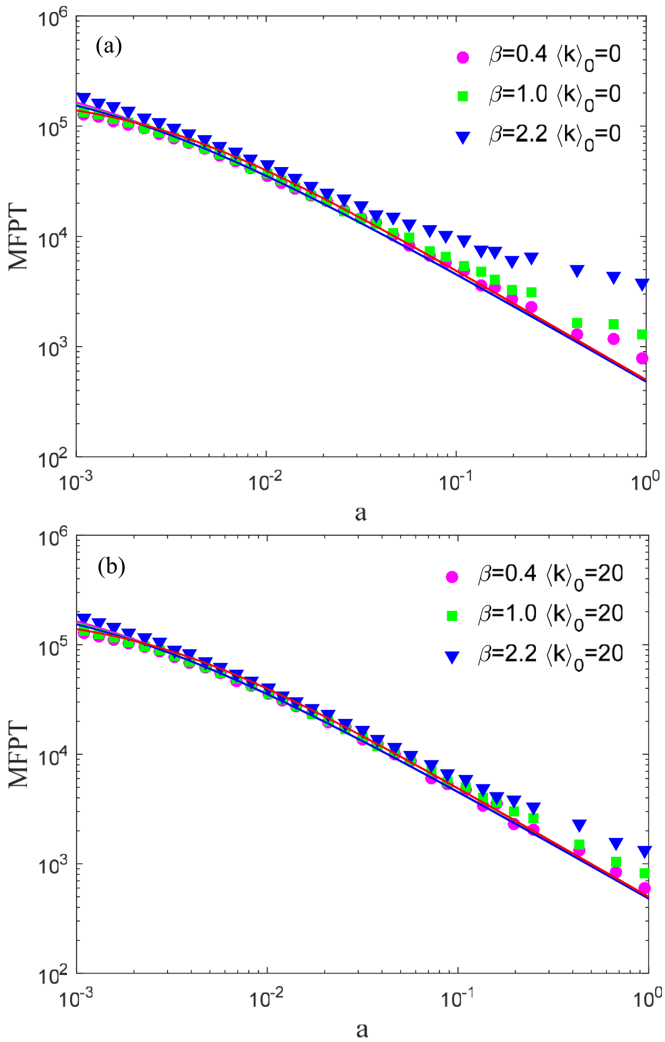

FIG. 5. The MFPT versus activity a for different β and $\langle k\rangle_0$. (a) $\langle k\rangle_0 = 0$; (b) $\langle k\rangle_0 = 20$. Solid curve represents analytically results without [Eq. (19) and with Eq. (17)] memory. Symbols represent simulations for different values of β with $\beta = 0.4, 1.0, 2.2$. The parameters are set as $N = 3000$ and $W = 1$. Each point is the average results over 100 realizations.

The distinction of theoretical solution between the MFPT with memory (black curve) and without memory (red curve) is not very obvious, even for large β with $\beta = 2.2$. For small β, the degree of nodes with activity a should be larger than that for large β, unfortunately, due to the omission of the new edges, node's degree are less than the actual situation. Therefore, theoretically, it is hard to accurately distinguish the degree value between different β, leading to the unobservable difference for the MFPT between the memory and memoryless cases.

Next we explore how the memory strength β affects the MFPT under different conditions of $\langle k\rangle_0$, i.e., extremely small $\langle k\rangle_0$ with $\langle k\rangle_0 = 0$ [Fig. 5(a)] and large $\langle k\rangle_0$ with $\langle k\rangle_0 = 20$ [Fig. 5(b)]. Independent of the average degree $\langle k\rangle_0$, the MFPT increases with β in Fig. 5. In other words, strong memory will delay the reachability of walkers. It can be understood as that for larger β, the reinforcement mechanism of edges generated by strong memory effect leads to the formation of clusterlike structure in the network, consequently, walkers are easier to get trapped at the traversed nodes and hardly to jump to new nodes. Thus, the presence of clusters of mutually interconnected nodes increases the MFPT, especially for the nodes with large activity a. The time of network evolution t_0, represented by the average degree $\langle k\rangle_0$, affects the derivation between simulation results and theoretical results. Larger $\langle k\rangle_0$ will shorten the gap between them. Thus, we expect that for sufficiently large $\langle k\rangle_0$, for any $\beta > 0$, the simulation for the MFPT will recover the theoretical results.

V. RANDOM-WALKS PROCESS IN REAL NETWORKS

We further investigate how an individual's memory affects the random-walk process in real networks. We collect the interactions containing time-stamped information between 30 398 Digg users in August 2008 via the 87627 reply network [37]. The Digg-Reply data are time varying, where each node describes a user and each time-resolved link denotes that a user replied to another user. Since many users tend to interact with the users in same group for multiple times, the social network is obviously driven by non-Markovian human dynamics.

In order to characterize an individual's memory in the network, we measure the activity a_i, defined as the fraction of interactions of node i per unit of time, which describes the propensity of node i to be involved in social interactions, is computed as $a_i = s_{i,\text{out}} \sum_j s_{j,\text{out}}$, where $s_{i,\text{out}}$ is the out-strength of node i integrated across the entire time span [16]. In Fig. 6(a), we performed a power-law distribution with exponential cutoff [38] on the Digg-Reply data set. Except for some data of the head, the activity distribution in the real data can be well fitted by the truncated power law distribution, indicating that the node's activity distribution in Digg-Reply data set is less heterogeneous.

We adopt a binning method to divide the nodes in total number, $N_b = \sum_{\text{agr}=1}^{N_{\text{act}}} N_{\text{deg}}(\text{agr})$, of activity-degree classes according to their activity a and the final degree k [32]. N_b represents the total number of groups. N_{act} represents the number of groups by activity. $N_{\text{deg}}(\text{agr})$ represents the number of groups divided by degree for activity group "agr." In detail, we first divide the nodes into N_{act} groups according to their activity. Since nodes with the same activity may feature different memory behavior in each activity group "agr," we group nodes by the final degree k into a total of $N_{\text{deg}}(\text{agr})$ groups.

Next, we define the probability for a node with degree k to get a new connection, $f_b(k)$, as:

$$f_b(k) = \frac{n_b(k)}{e_b(k)}, \tag{20}$$

where $e_b(k)$ denotes the total number of events engaged by the nodes of the bth class with degree k, and $n_b(k)$ represents the total number of events that nodes in bth group for degree k performed toward a new node. As shown Fig. 6(b), for curves with small activity category (bottom curves), the probability to attach to a new node quickly drops to 0, resulting in a small degree with $k \lesssim 10$. Nevertheless, for large activity category (top curves), even with very large degree ($k \sim 10^2$), the probability is nontrivial with $p(k) \gtrsim 0.1$.

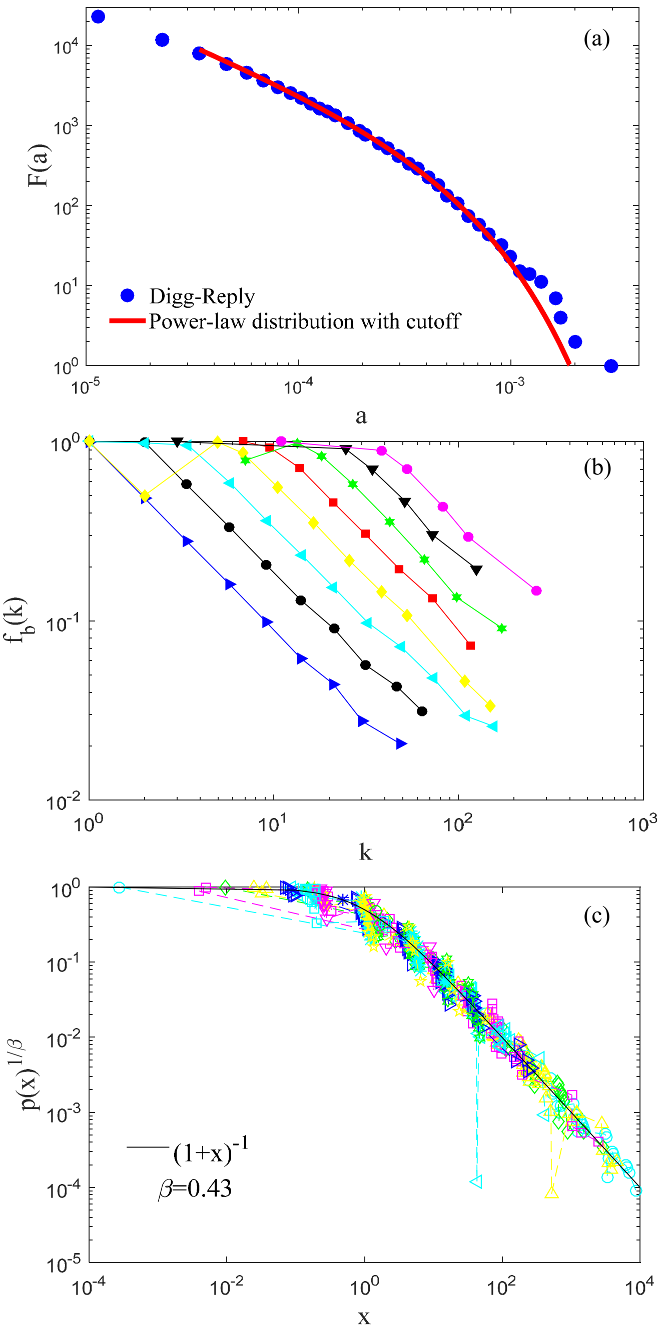

FIG. 6. Statistical properties in Digg-Reply data set. (a) The experimental activity distribution $F(a)$ in the Digg-Reply data set. The blue filled circles represent the real data. The red solid line represents the fitting result of the power-law distribution with exponential cutoff, $ca^{-\gamma}e^{-\lambda a}$, where $c = 9.984\times10^{-2}$, $\gamma = 1.117$, and $\lambda = 2476$. The cofficients with 95% confidence bounds, the nodes with activity $a > a_{\min}$ are chosen because it can obtain a smaller error, $a_{\min} = 3.42\times10^{-5}$. (b) The probability that nodes establish a new connection as a function of their degree. Each data sequence (different colors and markers) corresponds to selected nodes of the system, with the average activity of the nodes increasing from the bottom curves to the upper curves. (c) We rescale the attachment rate curves of all the nodes by setting $k \to x_b = k/c_b$ and plot $f_b(x) \to p_b(x) = f_b(x)^{1/\beta}$ versus x_b, where β is same for each colored curve. The memory strength is fitted as $\beta = 0.43$.

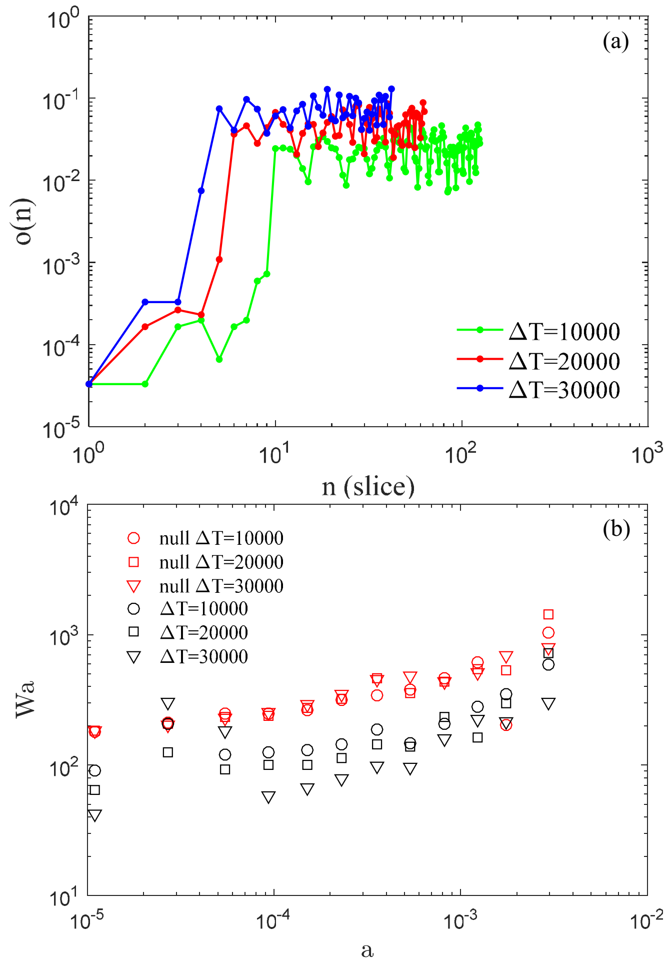

FIG. 7. Random-walk process in Digg-Reply data set. (a) The fraction of active nodes for different choices of time slice ΔT. (b) The distribution of W_a in the Digg data set (black) and in the null model (red) for different window size $\Delta T = 10\,000, 20\,000, 30\,000$ with $\frac{W}{N} = 200$. Each point is the average over 2000 independent simulations.

Then we use function $p_b(k, \beta) = [1 + \frac{k}{c(b)}]^{-\beta}$ to fit $f_b(k)$ by assuming that an individual's memory strength in the network obeys a power-law distribution. We measure the reinforcement process in the Digg-Reply network by minimizing the function $\chi^2(\beta)$ [32]:

$$\chi^2(\beta) = \sum_{b=1}^{N_b} \chi_b^2(\beta) = \sum_{b=1}^{N_b} \sum_{k=1}^{k_b} \frac{[f_b(k) - p_b(k, \beta)]^2}{\sigma_b(k)^2}, \quad (21)$$

where $\sigma_b(k) = \sqrt{\frac{f_b(k)[1-f_b(k)]}{e_b(k)}}$ is the STD of $f_b(k)$. We can obtain the optimal β in the Digg-Reply data set, i.e., $\beta = 0.43$. By scaling $k \to x_b = k/c_b$ and $f_b(x) \to p_b(x) = f_b(x)^{1/\beta}$, we obtain Fig. 6(c). We see that when the number of an individual's acquaintances is large, the probability of connecting with a new node is small. Thus, we see that $p_b(x)$ decreases with degree x.

In order to compare the effect of memory, we need to randomize the network to remove the memory effect and take it as the null network. Randomization is performed by recombining the interactions at each timestamp in order to remove the memory effect, while retaining the order of activation time for each node, the integration degree distribution for the final time, and the degree distribution at each time step [39].

To explore the effect of the number of active nodes on random walks, we divide the original data according to the time interval $\Delta T = 10\,000, 20\,000, 30\,000$, respectively. As can be seen from Fig. 7(a), with the increase of time interval ΔT, the number of active nodes in the time accumulated network increases accordingly. In Fig. 7(b), we compare the distributions of walkers W_a versus activity a on the data network with the null network for different time interval ΔT. In the null model, since the randomization process eleminates the effect of memory, W_a is hardly affected by ΔT. Compared with the null model, strong ties established by memory in the real data lower W_a for all the time slices ΔT we tested, which are consistent with our results on artificial networks. Due to the lower heterogeneity of node's activity in Digg-Reply network, the number of walkers fluctuates less with node's activity, thus, we see a flat increase in W_a.

VI. DISCUSSION AND CONCLUSION

In this work, we investigated the random-walk process on temporal networks with memory and explore how an individual's memory and the starting time of the diffusion coaffect the random-walk process unfolding on the network. Under the assumption of network evolution for long time, we derived analytical expressions of the distribution of walkers and the MFPT at the stationary state.

Monte Carlo simulation results show that, compared with the memoryless case, with the introduction of memory, it enhances the activity fluctuation and leads to the formation of small clusters of mutual contacts within high activity nodes, resulting in a slower increase of the average degree. Thus, nodes' abilities of collecting walkers are weaker than that in the memoryless case. One the other hand, the reinforcement mechanism between link formation leads to the delay of the MFPT due to the fact that the walker is easier to get trapped at traversed nodes. Stronger memory further strengthens the effect. The time for network evolution before the random-walk process, measured by the average degree $\langle k \rangle_0$, plays a trivial role in the distribution of walkers, W_a, while it greatly affects the MFPT. Numerical results show that the MFPT converges toward the analytical prediction as $\langle k \rangle_0$ becomes large. We performed similar analysis on real networks, which is consistent with the results of the artificial networks. The effect of the heterogeneity of the activity distribution on random-walk process has been verified in Ref. [14]. It shows that the difference of collecting walkers between nodes with small activity and nodes with large activity is reduced in homogeneous networks. We also find similar results in real network data.

In conclusion, our work provides a comprehensive view for the random-walk process in temporal networks with memory, compared to that in memoryless case. In the presence of memory, the number of walkers decreases at steady state and the MFPT gets larger than that of the memoryless case. Moreover, the effect of an individual's memory on the random walks in real data verifies the results on the artificial networks. As a possible future work, memory can be incoroperated with diverse individual behavior, such as higher interaction, in time-varying networks.

ACKNOWLEDGMENTS

This work was supported by the National Key Research and Development Program of China under Grant No. 2017YFE0117500, No. 2020YFB0704503, No. 2018YFB0704400, and No. 2018YFB0704402, the National Natural Science Foundation of China under Grant No. 91746203, Natural Science Foundation of Shanghai under Grant No. 20ZR1419000.

[1] D. F. Gleich, Pagerank beyond the web, SIAM Rev. **57**, 321 (2015).
[2] M. Rosvall and C. T. Bergstrom, Maps of random walks on complex networks reveal community structure, Proc. Natl. Acad. Sci. USA **105**, 1118 (2008).
[3] J. I. Gold and M. N. Shadlen, The neural basis of decision making, Annu. Rev. Neurosci. **30**, 535 (2007).
[4] L. Lovász, L. Lov, and O. Erdos, Random walks on graphs: A survey, Combinatorica, 1 (1996).
[5] C. Domb, Self-avoiding walks on lattices, Adv. Chem. Phys. **15**, 229 (2007).
[6] A. Fronczak and P. Fronczak, Biased random walks in complex networks: The role of local navigation rules, Phys. Rev. E **80**, 016107 (2009).
[7] S. E. Venegas-Andraca, Quantum walks: A comprehensive review, Quantum Inf. Proc. **11**, 1015 (2012).
[8] K. T. D. Eames and M. J. Keeling, Modeling dynamic and network heterogeneities in the spread of sexually transmitted diseases, Proc. Natl. Acad. Sci. USA **99**, 13330 (2002).
[9] M. E. Newman, A.-L. E. Barabási, and D. J. Watts, *The Structure and Dynamics of Networks* (Princeton University Press, Princeton, NJ, 2006).
[10] A. Curci and B. Rimé, The temporal evolution of social sharing of emotions and its consequences on emotional recovery: A longitudinal study, Emotion **12**, 1404 (2012).
[11] H. Kim and R. Anderson, Temporal node centrality in complex networks, Phys. Rev. E **85**, 026107 (2012).
[12] H. Kim, M. Ha, and H. Jeong, Scaling properties in time-varying networks with memory, Eur. Phys. J. B **88**, 315 (2015).
[13] N. Perra, B. Gonçalves, R. Pastor-Satorras, and A. Vespignani, Activity driven modeling of time varying networks, Sci. Rep. **2**, 469 (2012).
[14] N. Perra, A. Baronchelli, D. Mocanu, B. Gonçalves, R. Pastor-Satorras, and A. Vespignani, Random Walks and Search in Time-Varying Networks, Phys. Rev. Lett. **109**, 238701 (2012).
[15] T. Hoffmann, M. A. Porter, and R. Lambiotte, Random walks on stochastic temporal networks, in *Temporal Networks* (Springer, Berlin, 2013), pp. 295–313.

[16] L. Alessandretti, K. Sun, A. Baronchelli, and N. Perra, Random walks on activity-driven networks with attractiveness, Phys. Rev. E **95**, 052318 (2017).

[17] M. Yang, B. Wang, and Y.-X. Han, Random walk on the activity-driven model with mutual selection, Europhys. Lett. **124**, 48004 (2018).

[18] A. Moinet, M. Starnini, and R. Pastor-Satorras, Random walks in non-poissoinan activity driven temporal networks, New J. Phys. **21**, 093032 (2019).

[19] A. Moinet, M. Starnini, and R. Pastor-Satorras, Burstiness and Aging in Social Temporal Networks, Phys. Rev. Lett. **114**, 108701 (2015).

[20] E. Ubaldi, A. Vezzani, M. Karsai, N. Perra, and R. Burioni, Burstiness and tie activation strategies in time-varying social networks, Sci. Rep. **7**, 46225 (2017).

[21] M. Nadini, K. Sun, E. Ubaldi, M. Starnini, A. Rizzo, and N. Perra, Epidemic spreading in modular time-varying networks, Sci. Rep. **8**, 2352 (2018).

[22] Y. Lei, X. Jiang, Q. Guo, Y. Ma, M. Li, and Z. Zheng, Contagion processes on the static and activity-driven coupling networks, Phys. Rev. E **93**, 032308 (2016).

[23] N.-N. Dong, Y.-X. Han, Q. Li, and B. Wang, Impacts of multi-type interactions on epidemic spreading in temporal networks, Int. J. Mod. Phys. C **31**, 2050020 (2020).

[24] A. R. Benson, D. F. Gleich, and J. Leskovec, Higher-order organization of complex networks, Science **353**, 163 (2016).

[25] J. Grilli, G. Barabás, M. J. Michalska-Smith, and S. Allesina, Higher-order interactions stabilize dynamics in competitive network models, Nature **548**, 210 (2017).

[26] I. Iacopini, G. Petri, A. Barrat, and V. Latora, Simplicial models of social contagion, Nat. Commun. **10**, 2485 (2019).

[27] K. Devriendt and P. Van Mieghem, The simplex geometry of graphs, J. Complex Netw. **7**, 469 (2019).

[28] A. Bellaachia and M. Al-Dhelaan, Random walks in hypergraph, in *Proceedings of the 2013 International Conference on Applied Mathematics and Computational Methods* (Venice Italy, 2013), pp. 187–194.

[29] K. Sun, A. Baronchelli, and N. Perra, Epidemic spreading in non-markovian time-varying networks, Technical report, 2014.

[30] L. Zino, A. Rizzo, and M. Porfiri, Modeling memory effects in activity-driven networks, SIAM J. Appl. Dynam. Syst. **17**, 2830 (2018).

[31] M. Karsai, N. Perra, and A. Vespignani, Time varying networks and the weakness of strong ties, Sci. Rep. **4**, 4001 (2014).

[32] E. Ubaldi, N. Perra, M. Karsai, A. Vezzani, R. Burioni, and A. Vespignani, Asymptotic theory of time-varying social networks with heterogeneous activity and tie allocation, Sci. Rep. **6**, 35724 (2016).

[33] M. Tizzani, S. Lenti, E. Ubaldi, A. Vezzani, C. Castellano, and R. Burioni, Epidemic spreading and aging in temporal networks with memory, Phys. Rev. E **98**, 062315 (2018).

[34] R. Lambiotte, V. Salnikov, and M. Rosvall, Effect of memory on the dynamics of random walks on networks, J. Complex Netw. **3**, 177 (2015).

[35] I. Scholtes, N. Wider, R. Pfitzner, A. Garas, C. J. Tessone, and F. Schweitzer, Causality-driven slow-down and speed-up of diffusion in non-Markovian temporal networks, Nat. Commun. **5**, 5024 (2014).

[36] S. Janson and Y. Peres, Hitting times for random walks with restarts, SIAM J. Discr. Math. **26**, 537 (2012).

[37] M. De Choudhury, H. Sundaram, A. John, and D. D. Seligmann, Social synchrony: Predicting mimicry of user actions in online social media, in *Proceedings of the 2009 International Conference on Computational Science and Engineering* (IEEE, Los Alamitos, CA, 2009), Vol. 4, pp. 151–158.

[38] A. Clauset, C. R. Shalizi, and M. E. J. Newman, Power-law distributions in empirical data, SIAM Rev. **51**, 661 (2009).

[39] M. Starnini, A. Baronchelli, A. Barrat, and R. Pastor-Satorras, Random walks on temporal networks, Phys. Rev. E **85**, 056115 (2012).